Title
Dispersion of buoyant emissions from low level sources in urban areas: water channel modelling

Journal
International Journal of Environment and Pollution, 52(3/4)

ISSN
0957-4352 1741-5101

Authors
Pournazeri, Sam
Schulte, Nico
Tan, Si
et al.

Publication Date
2013

DOI
10.1504/IJEP.2013.058460

Peer reviewed

Dispersion of buoyant emissions from low level sources in urban areas: water channel modelling

Sam Pournazeri, Nico Schulte and Si Tan

Department of Mechanical Engineering,
University of California Riverside,
Riverside, CA 92521, USA
E-mail: spournazeri@engr.ucr.edu
E-mail: nschulte@engr.ucr.edu
E-mail: sitan@engr.ucr.edu

Marko Princevac*

Department of Mechanical Engineering,
University of California Riverside,
Bourns Hall A359, Riverside, CA 92521, USA
E-mail: marko@engr.ucr.edu
*Corresponding author

Akula Venkatram

Department of Mechanical Engineering,
University of California Riverside,
Bourns Hall A343, Riverside, CA 92521, USA
E-mail: venky@engr.ucr.edu

Abstract: A laboratory study was done to investigate dispersion of buoyant emissions from near surface sources in urban areas. Ground level concentrations under different surrounding building geometries were measured using a newly developed system based on laser induced fluorescence. In the presence of upstream buildings AERMOD (AMS/U.S. EPA regulatory dispersion model) is unable to explain concentrations close to the source. Plume visualisations and velocity measurements show that upstream buildings induce low velocity and a highly turbulent region near the stack, which increases the plume rise and induces rapid vertical mixing. Also, the urban canopy imposes a length scale on the horizontal turbulence, causing the plume to spread laterally with the square root of distance ($\sim x^{1/2}$) rather than linearly as occurs in open terrain. A Gaussian-based dispersion model which accounts for these effects performs substantially better in predicting ground level concentrations associated with buoyant emissions from distributed power generators in urban areas.

Keywords: AERMOD; air quality; buoyant emission; dispersion; distributed power generators; water channel.

Reference to this paper should be made as follows: Pournazeri, S., Schulte, N., Tan, S., Princevac, M. and Venkatram, A. (2013) 'Dispersion of buoyant emissions from low level sources in urban areas: water channel modelling', *Int. J. Environment and Pollution*, Vol. 52, Nos. 3/4, pp.119–140.

Biographical notes: Sam Pournazeri received his PhD in Mechanical Engineering at University of California Riverside in 2012 and his BSc in Mechanical Engineering at Sharif University of Technology, Tehran, Iran in 2008. His research area focuses on environmental fluid dynamics, urban dispersion and micrometeorology and atmospheric boundary layer.

Nico Schulte is a PhD student in the Department of Mechanical Engineering at University of California Riverside.

Si Tan is a PhD student in the Department of Mechanical Engineering at University of California Riverside.

Marko Princevac received his PhD in Mechanical Engineering at Arizona State University in 2003 and his BSc in Mechanical Engineering and Naval Architecture at the University of Belgrade, Serbia. He is interested in fundamental and applied fluid mechanics research – in particular, the application of fundamental turbulence concepts to studies in environmental flows. Currently, he is focusing on field experimental research on urban flows, specifically on urban dispersion and parameterisations of turbulence within urban canyons.

Akula Venkatram received his BS in Mechanical Engineering in 1971 from the Indian Institute of Technology, Madras, India, and his PhD in Mechanical Engineering from Purdue University, West Lafeyette, Indiana. His research area focuses on comprehensive modelling of systems governing air quality and theoretical aspects of small-scale dispersion.

1 Introduction

For many years, central power plants have been the dominant provider of electricity for residential and industrial users. The major benefit of centralised power plants is the low energy cost compared with small-scale power generation, which is usually located close to users and could result in high costs due to the cost of fuel transportation and generating technologies. Starting from 1970, centralised power plants no longer provide considerably cheaper energy, because the capital cost of these power plants per energy unit is now comparable to that of small power generators. Therefore, industries moved toward distributed power generation, also called on-site power generation. Distributed power generation is driven by small power plants (< 10 MW) located in the vicinity of the user (≈ 100 m). The western US energy crisis in 2000 and 2001 expedited this process. During this time schools, businesses and hospitals moved toward independence from central power plants by installing on site small scale power generators, known as distributed power generators (DGs) (Heath et al., 2005). DGs may serve a single home, neighbourhood, or business more efficiently and reliably than a centrally located power plant, and at a lower cost (Allison and Lents, 2002). These benefits and the continuing concerns about power reliability, quality, cost, and evolving technology have all contributed to the use of DG. Although DGs were beneficial for local industries by providing power independency and lower cost, they have a significant effect on air quality in urban areas especially at neighbourhood (up to 1 or 2 km) and street scale (less than ~100 to 200 m) (Britter and Hanna, 2003). Exhausts from DGs are hot and highly buoyant; however, as they are released within the city, in the vicinity of businesses, schools, restaurants and hospitals, they can be captured in the wake produced by surrounding buildings. The dispersion of these kinds of pollutants is complicated and is strongly affected by the complex geometry of the buildings in urban areas, and a thorough understanding of the street-scale flow and turbulence is required to model it.

Several studies have examined the impact of DGs on air quality at urban and regional scales. Allison and Lents (2002) found that total emissions associated with realistic DG scenarios with the lowest emission factors and high waste heat recovery are nearly comparable to those of central generated power plants. Heath et al. (2006) examined the air quality impact of DG units relative to central generating stations. They found that the air quality impact of DG units, quantified in terms of intake factors, the ratio between the amount pollutants inhaled by population to the amount of pollutants released, could be as much as 20 times that of central generating (CG).

Although these studies provide an insight into the problem, they mostly focused on the regional impact of these sources and did not directly address the impact of DG emissions on ambient ground level concentrations in the vicinity of the source, which can be orders of magnitudes higher than the background pollutant concentrations. Motivated by this need the air quality modelling group at University of California, Riverside conducted several field and laboratory studies to address the question: How do DGs modify the ground level concentration pattern in urban areas at distances of 100 m from the stack?

Following this need, a tracer field study was conducted in Palm Springs, California, USA in Summer 2008 around a gas fired 650 kW DG unit (Jing et al., 2009, 2010; Venkatram et al., 2012; Pournazeri, 2012). Results from this study indicate that ground level concentrations associated with night-time measurements (i.e., neutral stability conditions) do not decrease rapidly with distance in comparison with daytime (i.e., unstable condition) observations. Also, observations show that nighttime concentrations are generally higher than daytime concentrations in the Palm Springs study, despite the large plume rise during the night. The main message driven from this field study was that the currently used dispersion models such as AERMOD are not able to describe the ground level concentrations from low-level buoyant sources in urban areas, especially during night-time where a neutral/stable boundary layer can limit the dispersion. The formulations of plume rise, plume spreads, and the micrometeorological parameters used in these models are designed primarily for large power plants without any building in the vicinity, and are thus not suitable for inhomogeneous urban areas. Therefore, there is a need to develop and apply methods to estimate the air quality impact of distributed generation at source-receptor distances of tens and hundreds of meters by developing new models for plume rise and dispersion from low level sources such as DGs. Due to the high costs and site-specific results of field studies, results from laboratory measurements can provide a thorough and cost effective insight into the problem. In this matter, wind tunnels and water channels play a major role in providing supplementary data to support the datasets from tracer field studies during model development.

There have been many water channel and wind tunnel studies done over the past years to investigate the effect of buildings on ground level concentrations. Macdonald et al. (1998) has investigated the plume dispersion in an urban model using a wind tunnel. It has been shown that both the lateral and vertical plume spreads in the presence of buildings are almost two to four times higher than cases where no buildings were present. Also, concentration profiles can be very well described by a simple Gaussian dispersion model at downwind distances beyond two rows from the building array. However, at short distances from the stack, substantial variations in the concentration profile were observed, which could not be explained through a Gaussian model. Gailis and Hill (2006) simulated the mock urban setting test (MUST; Biltoft, 2001) inside a wind tunnel and found that the narrow street induces channelling and less mixing along the wind direction. Numerical models such as the k-epsilon model FLUENT have also been used to model dispersion near buildings. One such study by Flowe and Kumar (2000) showed that FLUENT can be used to simulate flow over a building; their simulations showed that the cavity length highly depends on the upstream building height and width. They also examined the concentration within the recirculation zone downwind of the building.

Although all these studies provide valuable information on the impact of buildings on the ground level concentration from sources close to the ground, none of them addresses the question of how effectively buildings can modify the dispersion pattern when highly buoyant plumes are released in a built environment, since unlike the passive releases, these emissions can escape the urban canopy in a very short distance from the source. Although the Palm Springs field study has provided valuable information on dispersion from a distributed generator in a real urban setting, it is limited by the fact that its results are specific to the site geometry and the meteorological conditions of the field study. Furthermore, the concentration measurements were made at distances at which the plume from the generator had spread above the average height of the buildings, so the field concentration measurements do not directly reflect building effects, which might result in relatively high concentrations close to the source. In order to explain the dispersion behaviours observed in the field study, it is useful to conduct simulations in a water channel where the site geometry and selected meteorological parameters such as wind speed can be varied. The water channel simulations can also focus on dispersion close to the source where the flow and hence the plume is affected by the details of the building geometry. In this laboratory study, the effects of the surrounding building geometry on ground level concentrations associated with a modelled DG are investigated.

2 Laboratory setup

Simulated flows and emissions in water channels are the most efficient ways of studying the plume motion due to the relative simplicity of generating stably stratified flows and making visualisations using fluorescent dyes (Contini and Robins, 2001; Arya and Lape, 1990). Examples of such applications can be found in Hunter (1992), Ohba et al. (1990), Snyder (1985) and Hoult and Weil (1972) and will not be discussed here. Simulating flow and dispersion in water channels and wind tunnels requires utilising correct scaling techniques. These scaling methods are explained in more detail through another study by Pournazeri et al. (2012a). The laboratory study explained in this paper is conducted through a series of experiments in the water channel facility at the University of California Riverside, Laboratory for Environmental Flow Modelling (LEFM).

2.1 Water channel

A custom-designed circulating water channel with a test section that is 1.5 m long, 1 m wide, and 0.5 m deep [see schematic in Figure 1(a) and a photograph in Figure 1(b)] was used for the experiments. Water is circulated through the channel test section using a

15 kW axial pump, which produces a maximum mean velocity of 0.5 m s^{-1} in the test section. A variable frequency controller allows flow control with a resolution of 1/100 Hz, and a range of 0 to 60 Hz. Flow conditioning is achieved with profiled honeycombs and custom-built perforated screens. The perforated screens are used to generate desired inflow velocity profiles as a part of the flow conditioning. The channel flow is steady and becomes fully developed before reaching the test section. More details of the water channel setup can be found in Princevac et al. (2010).

Figure 1 (a) Water channel schematic (b) Water channel facility at University of California Riverside (LEFM) (see online version for colours)

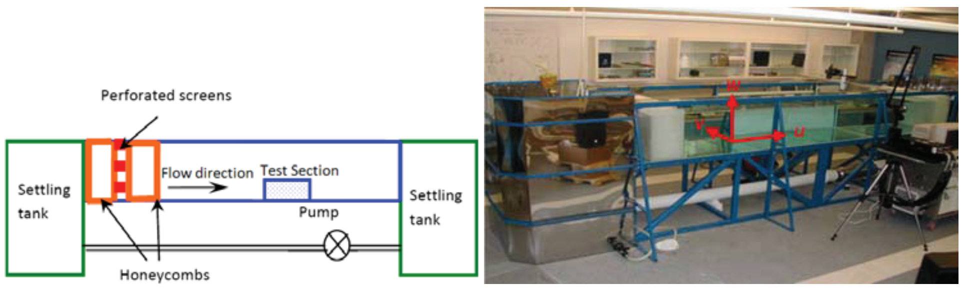

(a) (b)

2.2 Concentration measurements system

The existing concentration measurements system, planar laser induced fluorescence (PLIF), is one of the most powerful techniques to measure the tracer concentrations in water channels. The principle of this technique is relatively old and well addressed in literature (e.g., Hanson, 1988; Kychakoff et al., 1984; Pringsheim, 1949). This system consists of a 400 mJ Nd-YAG laser (Big Sky Laser Technologies Inc.) producing a 532 nm wavelength laser beam with a frequency of up to 15 Hz as the radiation source, a laser pulse synchroniser (TSI Inc.), a high resolution (1,600 × 1,192) POWERVIEW 2M CCD camera (TSI Inc.), and a 575-585 nm light filter. Rodamine B ($C_{28}H_{31}ClN_2O_3$) was used as a tracer dye. Derived from the Beer-Lambert law, the basic equation that relates the induced fluorescence intensity, I_f, with the fluorescent dye concentration is defined by Guilbault (1973) as

$$I_f = 2.3\phi I_0 \varepsilon bc \tag{1}$$

where the quantum efficiency ϕ is the ratio between the energy that is emitted to that absorbed, I_0 represents the laser light intensity, ε is the molar absorptivity, b is the absorption path length and c is the concentration of the fluorescent dye.

It was found that the PLIF results were reliable for the far field concentrations – in this study, far field refers to distances of greater than ten stack heights downwind from the stack where concentration gradients are relatively small (Huber and Snyder, 1982). However, measurements close to the source were highly biased, possibly due to the following four reasons:

1 light reflection from the water channel bottom face – this is especially pronounced when the goal is to measure near surface concentrations

2 laser light attenuation by varying plume intensity outside of the region of interest

3 self-illumination – this is very pronounced when extreme concentration gradients are present like in the case of near source measurements of ground level concentrations for an elevated release (here ground level concentration near the stack can be four orders of magnitude less than those nearby the stack)

4 averaging time – this is a problem of the recirculating nature of the tank.

Once dye recirculates back to the test section of the water channel, the background concentration becomes comparable to the ground level concentration. The dye recirculates back to the test section immediately after it is released from the stack. For these reasons we decided to keep PLIF for far field concentration measurements and to conduct near source measurements using a different technique.

The solution we used to overcome PLIF deficiencies was to use sampling probes that transmit the laser light to individual measurement locations. Each sensor probe consists of two 750 μm unjacketed plastic optical fibres: one for delivery of the laser beam to the measurement point and the second for delivering fluorescence light back to the CCD camera. Conducting the laser beam through short optical fibres prevented attenuation, and allowed us to direct the laser beam to a point, which avoids light reflection and self-illumination, and several sensors are placed in the background for real time corrections of the background concentrations to allow for longer averaging time. It has been experimentally shown that the best arrangement for the fibres in the sensor happens when the fibres are adjusted at an angle of 26° to each other (Kulchin et al., 2007). A sensor photo is given in Figure 2(a), and a schematic of the setup is given in Figure 2(b). The laser beam is focused on a bundle of optical fibres and each fibre guides laser light to the location of interest. Light from the fluorescence dye at the sensor location is then conducted to the camera via a second pair of fibres, referred here as return fibres. Return fibres are sparsely fixed in front of a CCD camera at predetermined locations so that all fibres are recorded at the same image without interference. A filter is placed in front of the camera to prevent any laser light reaching the CCD. Each sensor has to be individually calibrated. By utilising this system we sacrificed the whole plane PLIF measurements and replaced it with numerous point measurements. This is not a big disadvantage since sensors are inexpensive, small enough not to disturb the flow so that many of them can be placed in the desired region, and light intensities from all sensors are collected to a single image so that processing is relatively simple. Figure 3 shows the experiment setup for sensors, camera and laser. We conducted several experiments to validate the fibre optic system described in this paper. It was found that the concentration measurements obtained from optical fibre system compare well with those from the PLIF method, but the results have not been published. We also compared the results of the optical fibre method with concentrations measured in the far field from the stack in the Palm Springs field study and found that the order of magnitude of the concentrations is the same.

Figure 2 (a) Optical fibre sensor (b) Schematics of the concentration measurement system (green fibres are emitting fibres and red fibres are receiving fibres) (see online version for colours)

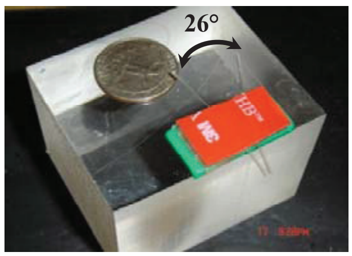

(a)

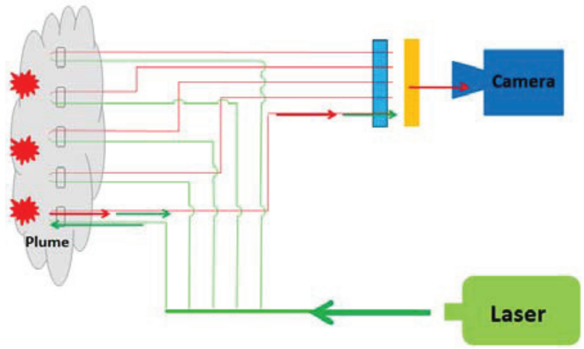

(b)

Figure 3 (a) Sensors placement in the water channel (b) Laser setup (c) Camera setup (see online version for colours)

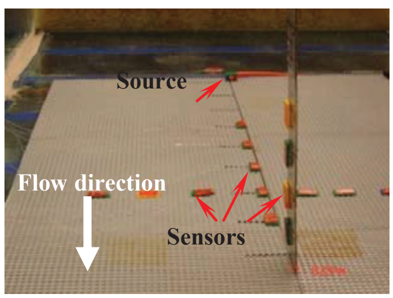

(a)

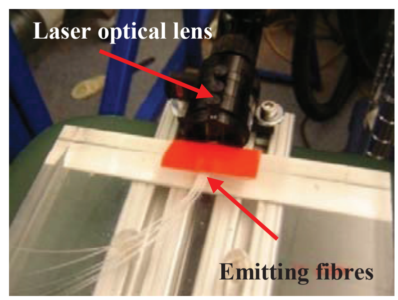

(b)

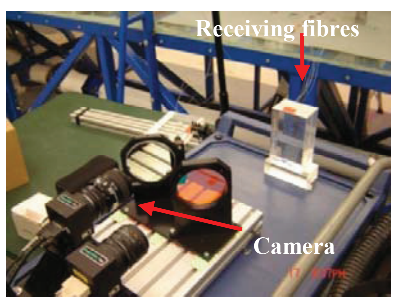

(c)

2.3 Velocity measurement system (PIV)

The velocity field is measured by TSI's particle image velocimetry (PIV) system. This system uses the same laser system as the concentration system in addition to a PowerView Plus 2M and 11M camera. Pliolite Ultra 100 particles are used as seeding particles. In order to measure the fluid's velocity, at least two separate exposures must be recorded. This typically involves producing a pair of laser pulses which are recorded onto a pair of camera frames. The frames are then split into a large number of examination areas, often called tiles. Through image processing it is then possible to calculate a displacement vector for each tile. This displacement is converted to a velocity using the time step between consecutive images (in our case Δt = 1.2 ms). Insight 3G (TSI Inc.) software is used for data collection and image processing. The PIV measurement technique is well established and widely used for fluid flow investigations (Adrian, 1988, 1991, 1997; Prasad et al., 1992).

2.4 *Plume visualisation technique*

We studied plume rise and spread in the water channel using a plume visualisation technique. This simple technique consists of a commercial camera (Sony 4.1MP Cyber shot) located on a tripod and a light source illuminating the test section. By adjusting the lens aperture and/or shutter speed we achieve the desired exposure time and capture an average snapshot of the plume. Fluorescent dye, Uranine, is used as the visualising dye as it has high light intensity in the range of visible light. Therefore, plume visualisation can be achieved by releasing the tracer dye from the source and capturing a long exposure image for 30 s. This technique gives us an averaged visualisation image, which can be used to examine the plume behaviour under different meteorological conditions and building geometries. Figure 4 shows some examples of plume visualisation images achieved using this technique.

Figure 4 Plume visualisations for (a) palm springs DG model and (b) single stack non-buoyant release (see online version for colours)

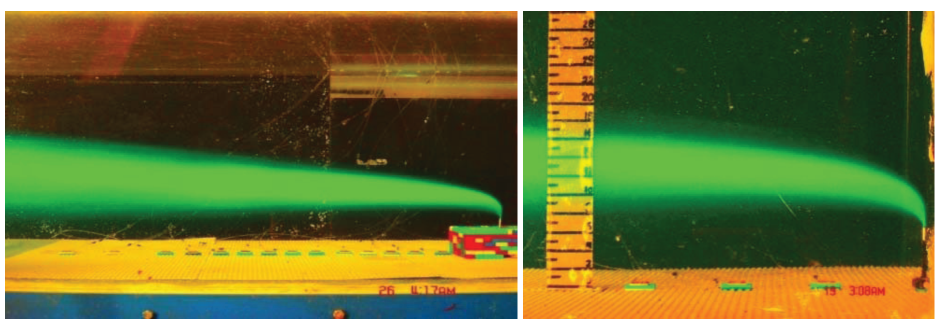

(a) (b)

2.5 *Experimental configuration*

As mentioned earlier, the main objective of this study is to investigate the impact of DGs on air quality in urban areas within short source-receptor distances. In order to do so, the Palm Springs DG building (15 m × 15 m × 7 m (*L* × *W* × *H*)) and stack with height of 9.3 m above ground level were modelled in the water channel at 1:100 scale. The stack temperature of 430 K, stack exit velocity of 10 m s^{-1}, and average wind speed of 2.5 m s^{-1} were considered as the corresponding field parameters.

Using the PIV system, flow velocities in the water channel with the pump frequency of 17.5 Hz were measured. Velocity data shows a horizontal free stream velocity of v_∞ = 45 mm s^{-1}, surface friction velocity of $u_* = 3.4$ mm s^{-1}, and average vertical turbulent velocity (σ_w) of 5.6 mm s^{-1} (i.e., vertical turbulent intensity of I_z = 0.12). The reference Reynolds number, based on the free stream velocity (v_∞) and characteristics building frontal length scale, H_b^* (length scale based on the obstacle frontal area; $H_b^* = (WH)^{1/2}$) was Re = 4,600, which is sufficient to satisfy Reynolds number independency criteria of $Re \approx 4{,}000$ (Halitsky, 1968; Fackrell and Pearce, 1981; Snyder, 1981; Yee et al., 2006). Details on the scaling technique used for this specific problem can be found in Pournazeri et al. (2012a). A summary of experimental conditions obtained from this scaling technique are given in Table 1.

Table 1 Experimental parameters

Parameters	*Value*
Free stream horizontal velocity (v_∞)	0.045 m s^{-1}
Re (based on H_b^*)	4,600
Internal diameter of the stack (D)	3 × 10^{-3} m
Stack exit velocity (V_s)	0.19 m s^{-1}
Stack exit Reynolds number (Re_s)	570
Average vertical turbulent velocity (σ_w)	0.0056 m s^{-1}
Vertical turbulent intensity of flow ($I_z = \sigma_w / v$)	~0.12–0.14
Surface friction velocity (u_*)	0.0034 m s^{-1}
Roughness length of Lego blocks (z_0)	~6 × 10^{-4} m
Plume specific gravity (SG)	0.99

3 Results from urban dispersion measurements

In this set of experiments the effect of upstream buildings on the ground level concentration of buoyant emissions released from the DG has been investigated. As mentioned earlier, none of the current experimental studies addresses the question of how effectively buildings can modify the dispersion pattern when highly buoyant plumes are released in a built environment where, unlike the passive releases, these emissions can escape the urban canopy in a very short distance from the source. Therefore, a 3 × 2 array of equal height buildings has been created and situated upstream of the DG building. The photographs of the modelled DG and upstream buildings in the water channel are shown in Figure 5.

Figure 5 (a) DG and single storey upstream buildings and (b) DG and double storey upstream buildings modelled in water channel using Lego™ (see online version for colours)

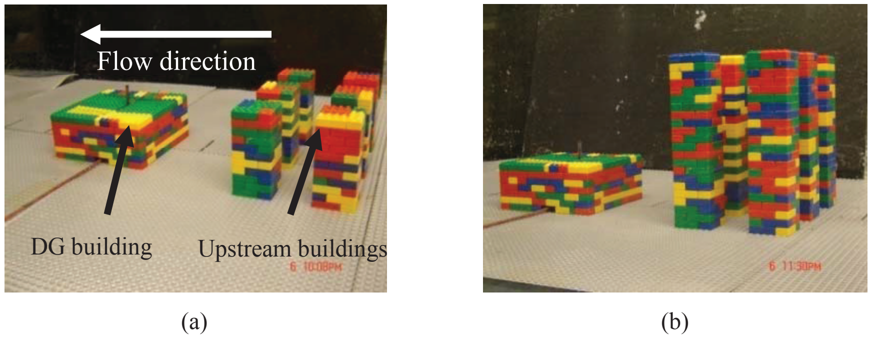

3.1 Ground level concentration measurements

Experiments regarding the air quality impact of DG have been done in three different cases:

1. DG with no upstream buildings
2. DG with upstream buildings the same height as the stack (single storey)
3. DG with upstream buildings of double the height of the stack (double storey).

The optical fibre system described in Section 2.2 was used to measure concentrations at 15 points located at ground level and from 0.25 m to 2 m from the stack. Results of concentration (C/Q where Q is the source mass flow rate) measurements are shown in Figure 6. Concentrations close to the source are comparable to the far field concentrations and the difference between the far field concentrations and the maximum concentrations becomes smaller as the height of the upstream buildings is increased. The location of the maximum concentration occurs at distances of five to seven stack heights (H_s) from the source. The concentration far from the stack does not change much going from no upstream buildings to single storey upstream buildings, but is reduced by about a factor of two when the double storey buildings are present. These results have been compared with predictions from AERMOD/PRIME (Cimorelli et al., 2005; Schulman et al., 2000) as shown in Figure 6. Comparison shows that AERMOD/PRIME predicts the concentration associated with the single DG well, but it underestimates and overestimates concentrations associated with single and double storey upstream buildings, respectively, especially in the near field ($x \leq 10$ H_b). Although the PRIME model (an algorithm for modelling the effects of downwash) has been evaluated over many different building configurations (EPA, 2003), the model was not validated for multiple building geometries (Petersen and Beyer-Lout, 2012). The PRIME model (Schulman et al., 2000) was primarily designed to assess the impact of a single building on the dispersion and plume rise. In case the problem consists of a cluster of buildings, the building profile input programme (BPIP) calculates the height and width of an effective building and the position of the stack that simulates the Snyder and Lawson (1994) database flow region (i.e., the database that was used to develop the PRIME downwash algorithm; Petersen and Beyer-Lout, 2012). It can be hypothesised from the results shown in Figure 6 that for the case of double storey upstream buildings, the BPIP model locates the stack within the cavity of the effective building where the emissions released from the stack are trapped within the cavity. This explains why in the case of double storey upstream buildings there is a substantial overestimation of concentration. On the other hand, in the case of single storey upstream buildings, BPIP locates the stack out of the cavity which allows the emissions to escape the cavity and avoid downwash. As it can be seen, this study shows that neither of these two extreme scenarios occurs when the height of the upstream buildings is changed. It needs to be mentioned that these hypotheses need to be further investigated using additional model evaluation practices.

Figure 6 Effect of the presence of the upstream building on the normalised ground level concentration (C/Q) and predictions by AERMOD for (a) no upstream buildings, (b) single storey upstream buildings and (c) double storey upstream buildings (see online version for colours)

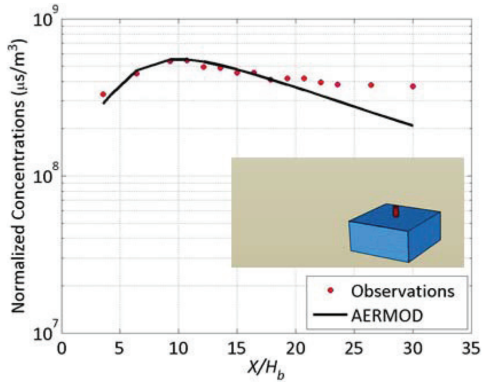

(a)

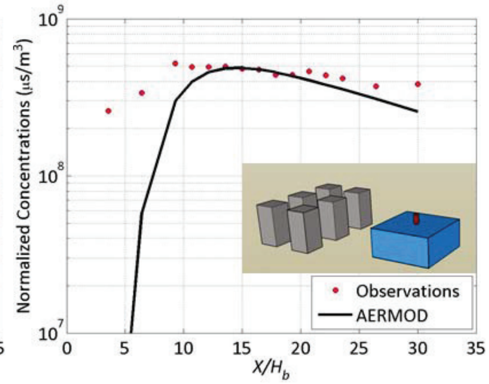

(b)

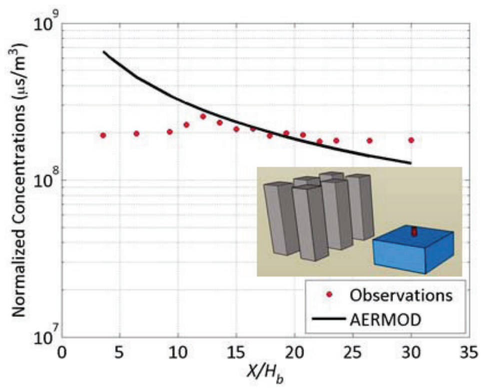

(c)

Note: Red dots (●) represent the observed ground level concentrations and solid black lines (▬) represent AERMOD predictions of ground level concentrations.

Figure 6 also shows that the presence of upstream buildings reduces concentrations close to the stack, however, as the height of the upstream buildings is increased (double storey) concentrations decrease much slower with downwind distance and the downstream concentration profiles flatten. In order to understand the reason for this strange behaviour, turbulence and velocity measurements as well as plume visualisation experiments have been conducted to investigate the effect of upstream buildings.

3.2 Turbulence and velocity measurements

Vertical profiles of velocity were measured for the three cases shown in Section 3.1. Each profile was taken at the position of the stack, and extended from above the top of the stack up to a height of 3.5 H_b. Measurements were not made below the stack height because the model building and stack located there would interfere with the measurements. Results from velocity measurements show that the presence of upstream buildings induces a low velocity as well as a highly turbulent region near the stack, and this effect becomes more significant when the height of the upstream buildings is increased (Figure 7). In the case with single storey buildings the wind speed is reduced by 30% and turbulent intensity is increased by 50% at the height of the stack compared with the case with no upwind buildings, and when there are double storey buildings situated upwind the wind speed is reduced by about a factor of two and the turbulent intensity is increased by a factor of two at the height of the stack. The change in wind speed and turbulent intensity persists up to a height of two building heights for the single storey buildings.

Figure 7 Laboratory velocity measurements in vicinity of the DG building under three different building geometry of only DG building (●),single storey upstream buildings (●) and double storey upstream buildings (●) for (a) mean stream wise velocity normalised by maximum velocity (0.045 m s^{-1}) and (b) vertical turbulent intensity (I_z) (see online version for colours)

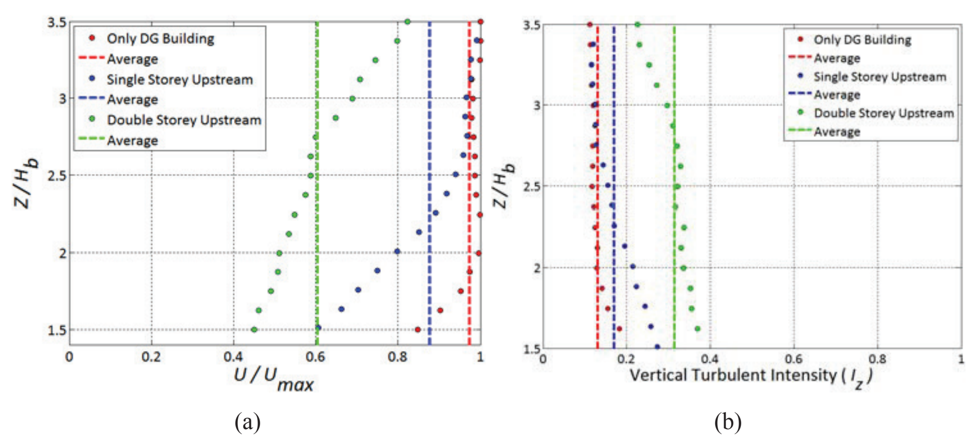

3.3 Vertical mixing

Vertical mixing induced by buildings has also been investigated by long exposure imaging of the plume released from the DG under different building geometries. Results from plume visualisation (Figure 8) indicate that upstream buildings decrease the wind speed near the stack, and this fact yields higher plume rise. However, at the same time, upstream buildings increase turbulent intensities near the stack resulting in stronger vertical mixing as compared to the case where there are no upstream buildings. The concentration depends on the ratio of the plume rise to the vertical plume spread, as modelled in equation (6). A higher plume rise lowers the ground level concentrations while increased vertical mixing increases ground level concentrations. Thus, the presence of buildings results in effects that counteract each other in changing the ground-level concentrations relative to the no upstream building case. According to Briggs (1984), plume rise can be parameterised as,

$$h_p = \left(\frac{3}{2\beta^2} \frac{F_b x^2}{U^3} + \frac{3}{\beta^2} \frac{F_m x}{U^2} \right)^{1/3}, \tag{2}$$

where $F_b = g b_0^2 V_s \left(\frac{T_p - T_a}{T_p} \right)$ is the buoyancy flux parameter, $F_m = b_0^2 V_s^2$ is the momentum flux parameter, b_0 is the stack radius, V_s is the stack exit velocity, T_p and T_a are the exhaust plume and ambient temperatures, U is the wind speed, and x is the distance from the stack. With the given experimental parameters the plume rise is dominated by the buoyancy flux, so the plume rise scales as $h_p \sim U^{-1}$. The vertical plume spread, σ_z, is proportional to the turbulent intensity: $\sigma_z \sim (\sigma_w / U)x$, where (σ_w / U) is the turbulent intensity, which increases as the building height is increased. Using equation (2), a plume rise of about 3 cm at a distance of 25 cm from the stack was estimated when there are no buildings placed upwind of the DG building. When the single storey buildings are placed upstream the plume rise is larger, and the plume likely rises above the top of the region where the wind speed and turbulent intensity are modified by the upstream buildings, which occurs at about 16 cm above ground level (see Figure 7). When double storey buildings are placed upwind, the wind speed and turbulent intensity are changed up to a larger height, so the plume is always contained within a region where the wind speed is reduced and turbulence is increased. This explains why the reduction in concentrations due to the presence of the single story buildings is much smaller than that of the double story buildings: the wind speed and turbulent intensity at the plume centreline is not significantly changed from the no building configuration to the single story building configuration, so the plume rise and spread is similar far from the stack for no building or for a single story building. The wind speed is significantly reduced and the turbulent intensity is increased for the double story configuration, so the plume spread is increased when there are double story buildings, and the concentration is reduced. This shows that source height can have a significant impact on ground level concentrations when the stack exit is near the top of the urban canopy layer (UCL).

3.4 Plume lateral spread

In order to investigate lateral spread of a plume released from low level sources (below the canopy layer height) inside the urban area, the modelled stack was placed in a 5 × 5 array of buildings with heights slightly higher than the stack height in order to make sure that the plume is released within the urban canopy. Plume visualisation was used to observe the averaged lateral spread of the plume. Figure 9 shows the laboratory setup for this experiment.

Figure 8 DG and upstream buildings modelled in water channel using Lego™ and plume visualisations for (a) no upstream buildings, (b) single storey upstream buildings and (c) double storey upstream buildings (see online version for colours)

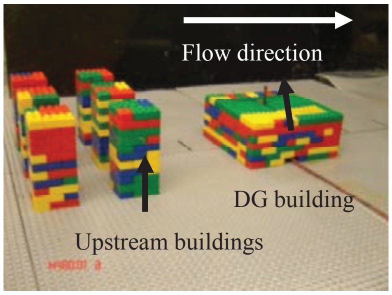

(a)

(b)

(c)

(d)

Figure 9 Laboratory setup for plume lateral spread visualisation, (a) 5 × 5 arrays of buildings (b) camera configuration with respect to buildings and stack (see online version for colours)

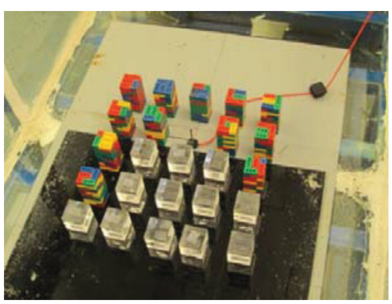

(a)

(b)

Figure 10 shows the visualisation of plume lateral spreads with and without buildings. As can be seen in Figure 10, the lateral spread in the absence of buildings increases linearly with distance and is higher than that in the presence of buildings. The presence of buildings results in rapid initial mixing (as compared to no building scenario) followed by a relatively slow spread that is close to $\sim x^{1/2}$ behaviour, where x presents the stream wise distance from the source. These results indicate that buildings reduce the effects of meandering on plume spread, and at the same time impose a length scale on the horizontal turbulence. This length scale gives rise to the observed $x^{1/2}$ behaviour. The effect of buildings on lateral plume spread can be modelled through the following expression

$$\sigma_y^2 = \left(\frac{(\sigma_v / U)x}{(1 + x / L_b)^{1/2}} \right) + \sigma_{y0}^2, \tag{3}$$

where σ_y is the horizontal plume spread, σ_v is the standard deviation of horizontal velocity fluctuations, σ_{y0} is the initial horizontal spread, and L_b is the length scale associated with the urban geometry. It is hypothesised that the length scale dominating the horizontal dispersion of the plume is proportional to the width of the buildings or the span wise distance between the buildings (Belcher, 2005). We tentatively chose W_b (width of the buildings), while the distance between the buildings may also be a valid choice. In this study, the distance between buildings equals their width, so both choices result in the same model results. L_b becomes infinity in the absence of buildings. The dependence of the horizontal scale of turbulence on building dimensions is similar to the formulation proposed by Belcher (2005). We also take the initial spread of the plume to be $W_b / \sqrt{2\pi}$. When $x >> L_b$, equation (3) yields square root growth of lateral spread,

$$\sigma_y^2 = \left(\sigma_v (xL_b)^{1/2} / U \right)^2 + \sigma_{y0}^2 \tag{4}$$

Figure 10 Plume lateral spread visualisation for (a) with buildings and (b) without buildings; (c) comparison of lateral spread (σ_y) for with/without buildings (see online version for colours)

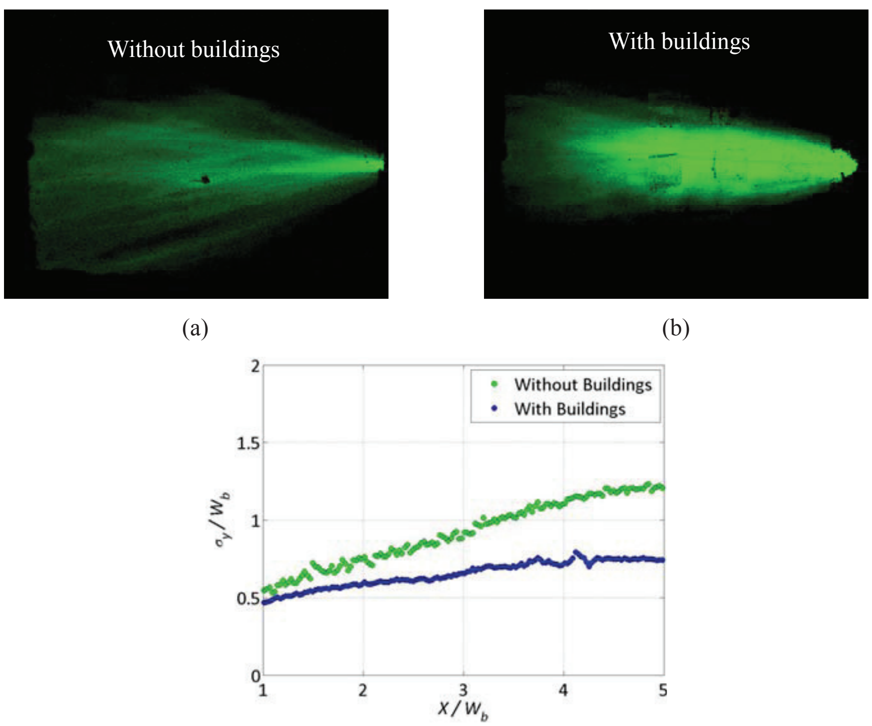

(a) (b)

(c)

Figure 11(a) shows a schematic of the plume lateral spread in the presence of buildings and Figure 11(b) shows the comparison between the proposed model [equation (3)] and the observations from the water channel simulation. It is seen that the model predicts the lateral spread well using the measured turbulent intensity.

Figure 11 (a) Schematic of plume lateral spread (σ_y) in the presence of buildings, W_b represents the averaged width of the buildings (b) Measured plume lateral spread in case of presence of buildings (blue dots ●) and absence of buildings (green dots ●) and the comparison with the suggested model (black solid line ▬) (see online version for colours)

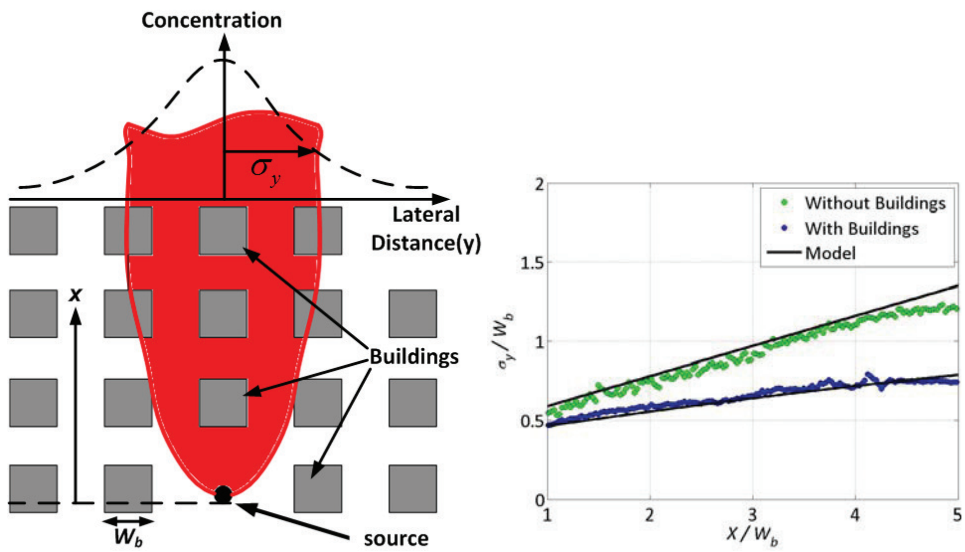

(a) (b)

4 Model modification

According to the video visualisation of plume obtained from the water tank experiment, it has been seen that buildings tend to induce more turbulence and increase vertical mixing. These video visualisation showed that in the presence of buildings part of the emission released from the stack is trapped within the UCL and gets well mixed as a result of the higher turbulence levels (as compared to the no building scenario) present in this layer. It is also observed that mixing becomes more vigorous as upstream building height increases relative to the no-building scenario. Following the results obtained in Section 3.4, it is hypothesised that buildings enforce a length scale on the horizontal turbulence which dominates the horizontal spread of the plume. The analysis in Section 3.4 assumed that this length scale is proportional to the geometry of the buildings. In summary, the results from plume visualisations indicate the need to include the following physical features in modelling the dispersion from low level buoyant sources:

1 stronger vertical mixing of material within the urban canopy as compared to the mixing above the canopy layer

2 length scale for horizontal mixing within UCL is set by building morphology for near field dispersion [equation (4)].

Figure 12 Schematic of the modified Gaussian model (well-mixed model) (see online version for colours)

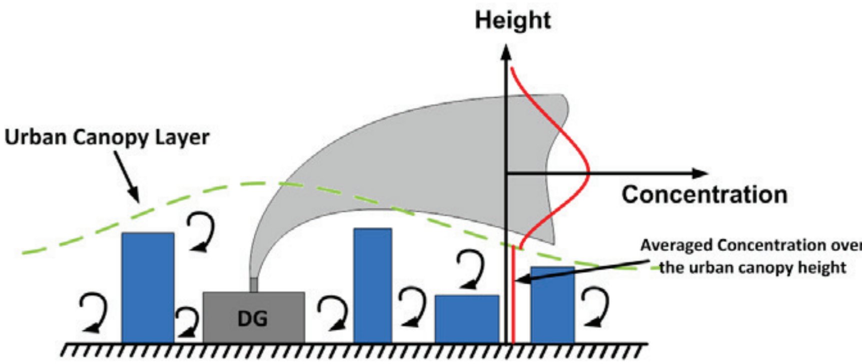

The two features of the building effects are illustrated by Figure 12, which shows the concentration profile from a modified Gaussian dispersion model over an urban area. The changes made to the Gaussian model are that the concentration is uniform over the height of the UCL due to vigorous vertical mixing and the horizontal plume spread is modified by the length scale proportional to the building morphology. The well mixed vertical concentration profile within the UCL is also used in other models such as PRIME (Schulman et al,. 2000). In this study only the ground level concentrations were measured. While the concentration should be described by the Gaussian model above the UCL, these measurements do not allow us to validate the shape of the concentration profile above the UCL. The effect of rapid vertical mixing within the urban canopy creates a uniform concentration with height, which can be modelled by assuming that ground level concentrations can be calculated by averaging the concentrations associated with the Gaussian dispersion model (including the reflection term) over the height of the UCL as follows:

$$C(x, y, 0) = \frac{1}{2\pi\sigma_y\sigma_z U} \exp\left(-\frac{y^2}{2\sigma_y^2}\right) \frac{1}{h_c}\int_0^{h_c}\left[\exp\left(-\frac{(z-h_e)^2}{2\sigma_z{}^2}\right)+\exp\left(-\frac{(z+h_e)^2}{2\sigma_z{}^2}\right)\right]dz \tag{5}$$

where U is the wind speed, h_e is the effective plume height, h_c is the height of the UCL (equivalent to average of buildings' heights) and σ_y, σ_z are the lateral and vertical spreads of the plume respectively. Equation (5) yields the analytical expression,

$$C(x, y, 0) = \frac{1}{2\sqrt{2\pi}\sigma_y U\ h_c} \exp\left(-\frac{y^2}{2\sigma_y^2}\right)\left[erf\left(\frac{h_e+h_c}{\sqrt{2}\sigma_z}\right)-erf\left(\frac{h_e-h_c}{\sqrt{2}\sigma_z}\right)\right] \tag{6}$$

In the modified model, the decrease of concentrations depends on the lateral spread, σ_y, which is a function of building dimensions in the urban canopy and is modelled through Equation (3). Plume rise is also calculated through the numerical plume rise model explained in Pournazeri et al. (2012b), where the effect of surrounding buildings as well as the effect of ambient turbulence is taken into account. Figure 13 shows a comparison of equation (6) with concentrations observed in the water tank. AERMOD/PRIME underestimates/overestimates the concentrations close to the source [Figures 13(b) and 13(c)], while the modified Gaussian model, Equation (6), provides a better description of the near field ($x \leq 10\ H_b$) concentrations. As shown in Figure 13, even though the well-mixed model shows better results than AERMOD in the near-field, it fails to capture the location of the peak ground-level concentration. Also, the well-mixed model predicts far-field concentrations better than the near-field concentrations in the double-story upstream building setup. These issues indicate the need for further investigation of the near field dispersion; more detailed analyses of the plume rise and vertical dispersion in the vicinity of buildings is needed.

Figure 13 Performance of AERMOD (black solid line ▬) and well mixed model (blue solid line ▬) explaining the ground level concentrations associated with buoyant emission in water channel (red dots ●) in the presence of (a) only DG building, (b) single storey upstream buildings and (c) double storey upstream buildings (see online version for colours)

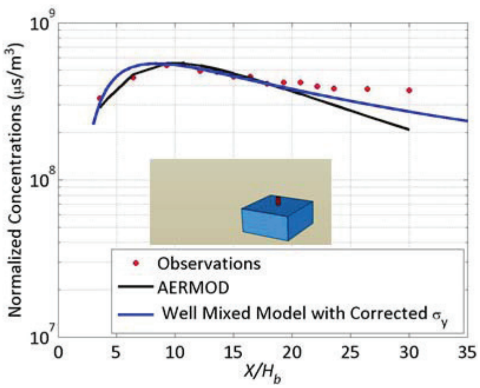

(a)

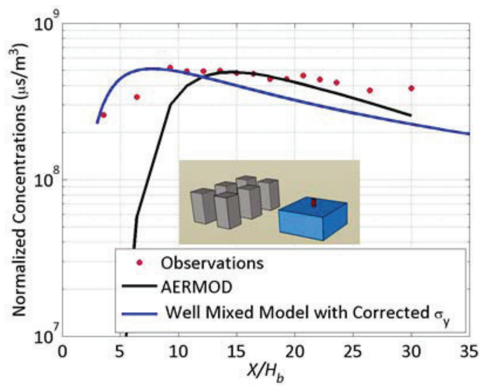

(b)

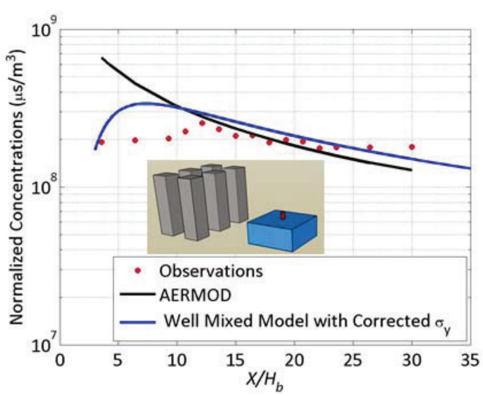

(c)

5 Summary and conclusions

Many of the previous laboratory studies on urban dispersion were focused on a passive plume released within a regular urban array, and there have almost been no studies done on the release of buoyant emissions from low-level sources in urban areas. In the introduction it was mentioned that it is important to investigate such sources because there are concerns that the rapid increase in the use of DGs in urban areas will likely have negative impacts on the air quality. In order to have better understanding on the dispersion process of DG emissions, laboratory simulations were conducted in a custom designed water channel. The Palm Springs DG was modelled in the water channel and tested under different surrounding building geometries. Ground level concentrations associated with a buoyant emission source were measured at different downstream distances. These data were used to evaluate the performance of the AERMOD/PRIME dispersion model at predicting ground level concentrations associated with these sources. It has been observed that AERMOD/PRIME performs well in the absence of surrounding buildings, but it tends to underestimate/overestimate ground level concentrations in the presence of single/double storey upstream buildings, respectively. Data from ground level concentration measurements was supplemented with data from velocity and turbulence measurements. Plume visualisation was also used to examine the behaviour of the plume in the presence of upstream buildings. Results show that upstream buildings can produce low velocity regions as well as high turbulence levels near the stack. The low velocity region allows the plume from the DG stack to rise higher and decreases the ground level concentration while high turbulence levels result in larger plume spread and increase the ground level concentration near the stack.

Lateral plume spread in an array (5 × 5) of buildings taller than the stack was also measured in the water channel. Results show that an urban building canopy imposes a horizontal length scale on lateral turbulence which is proportional to the building morphology within the canopy. Material released within the canopy first undergoes rapid horizontal spread proportional to the building width, and then spreads at a rate dependent on the lateral turbulent velocity within the canopy and the horizontal length scale set by the buildings. The horizontal spread within the canopy can differ substantially from that above the urban canopy.

These effects have been accounted for in a simple model which assumes that buildings in urban areas produce a highly turbulent boundary layer. Therefore pollutants released from low level buoyant sources entrain into this boundary layer and immediately get well mixed. The height of this canopy layer is highly dependent on the average height of the buildings in urban areas. The model for the horizontal plume spread assumes that the scale of the turbulence is determined by the building geometry, and allows the plume to spread with the square root of distance from the source in the presence of buildings. Comparisons between the model and laboratory observations show that the model gives an acceptable estimate of the concentrations especially at distances close to the source ($\leq 10\ H_b$). The encouraging results from this model suggest modifications to AERMOD to allow its application to buoyant low level releases in urban areas.

Acknowledgements

The authors are very grateful to three anonymous reviewers for careful review of the paper and helpful comments. This work was supported by the California Energy Commission; contract number CIEE MAQ-07-03.

References

Adrian, R.J. (1988) 'Review of particle image velocimetry research', *The Symposium on Optical Methods in Flow and Particle Diagnostics*, Paper presented at *6th International Congress on Applications of Lasers and Electro-Optics*, Vol. 9, pp.317–319, Optics and Lasers in Engineering, San Diego, CA.

Adrian, R.J. (1991) 'Particle-imaging techniques for experimental fluid-mechanics', *Annual Review of Fluid Mechanics*, Vol. 23, No. 1, pp.261–304.

Adrian, R.J. (1997) 'Dynamic ranges of velocity and spatial resolution of particle image velocimetry', *Measurement Science and Technology*, Vol. 8, No. 12, pp.1393–1398.

Allison, K.E. and Lents, J. (2002) 'Encouraging distributed generation of power that improves air quality: can we have our cake and eat it too?', *Journal of Energy Policy*, Vol. 30, No. 9, pp.737–752.

Arya, S.P.S. and Lape, J.F. (1990) 'A comparative study of the different criteria for the physical modeling of buoyant plume rise in a neutral atmosphere', *Atmospheric Environment*, Vol. 24A, pp.289–295.

Belcher, S.E. (2005) 'Mixing and transport in urban areas', *Philosophical Transactions of the Royal Society A*, Vol. 363, No. 1837, pp.2947–2968, doi:10.1098/rsta.2005.1673.

Biltoft, C. (2001) *Customer Report for Mock Urban Setting Test*, WDTC-FR-01-121 U.S. Army Dugway Proving Ground, Dugway.

Briggs, G.A. (1984) 'Plume rise and buoyancy effects', in Randerson, D. (Ed.): *Atmospheric Science and Power Production*, Chapter 8, pp.327–366, DOE/TIC-27601, DE84005177, U.S. Dept. of Energy Office of Sci. and Tech. Information, Springfield, VA.

Britter, R.E. and Hanna, S.R. (2003) 'Flow and dispersion in urban areas', *Annual Review of Fluid Mechanics*, Vol. 35, No. 1, pp.469–496.

Cimorelli, A.J., Perry, S.G., Venkatram, A., Weil, J.C., Paine, R.J., Wilson, R.B., Lee, R.F., Peters, W.D. and Brode, R.W. (2005) 'AERMOD: a dispersion model for industrial source applications. Part I: general model formulation and boundary layer characterization', *Journal of Applied Meteorology*, Vol. 44, No. 5, pp.682–693.

Contini, D. and Robins, A.G. (2001) 'Water tank measurements of buoyant plume rise and structure in neutral crossflows', *Atmospheric Environment*, Vol. 35, No. 35, pp.6105–6115.

EPA (2003) *AERMOD: Latest Features and Evaluation Results*, June 2003, EPA-454/R-03-003, USEPA Office of Air Quality, Planning and Standards, Research Triangle Park, North Carolina.

Fackrell, J.E. and Pearce, J.E. (1981) *Parameters Affecting Dispersion in the Near Wake of Buildings*, p.41, Report RD/M/1179N81, Central Electricity Generating Board, Marchwood Engineering Laboratories, UK.

Flowe, A.C. and Kumar, A. (2000) 'Analysis of velocity fields and dispersive cavity parameters as a function of building width to building height ratio using a 3-D computer model for squat buildings', *Journal of Wind Engineering and Industrial Aerodynamics*, Vol. 86, No. 2, pp.87–122.

Gailis, R.M. and Hill, A. (2006) 'A wind tunnel simulation of plume dispersion within a large array of obstacles', *Boundary-Layer Meteorology*, Vol. 119, No. 2, pp.289–338, doi: 10.1007/s10546-005-9029-1.

Guilbault, G.G. (1973) *Practical Fluorescence: Theory, Methods and Techniques*, Dekker, New York.

Halitsky, J. (1968) 'Gas diffusion near buildings', in Slade, D.H. (Ed.): *Meteorology and Atomic Energy*, TID-24190, Chapter 5-5, pp.221–231, National Technical Information Service, Springfield, Virginia.

Hanson, R.K. (1988) 'Combustion diagnostics: planar imaging techniques', Presented at *21st International Symposium on Combustion*, Vol. 21, pp.1677–1680, doi: 10.1016/S0082-0784(88)80401-6.

Heath, G.A., Granvold, P.W., Hoats, A.S. and Nazaroff, W.W. (2005) *Quantifying the Air Pollution Exposure Consequences of Distributed Electricity Generation*, Final Report to the University of California Energy Institute.

Heath, G.A., Granvold, P.W., Hoats, A.S. and Nazaroff, W.W. (2006) 'Intake fraction assessment of the air pollutant exposure implications of a shift toward distributed electricity generation', *Atmospheric Environment*, Vol. 40, No. 37, pp.7164–7177.

Hoult, D.P. and Weil, J.C. (1972) 'Turbulent plume in a laminar cross flow', *Atmospheric Environment*, Vol. 6, No. 8, pp.513–530, doi: 10.1016/0004-6981(72)90069-8.

Huber, A.H. and Snyder, W.H. (1982) 'Wind tunnel investigation of the effects of a rectangular-shaped building on dispersion of effluents from short adjacent stacks', *Atmospheric Environment*, Vol. 16, No. 12, pp.2837–2848, doi:10.1016/0004-6981(82)90034-8.

Hunter, G.C. (1992) *The Behavior of Plumes from Point Sources in Stratified Flows*, 275p, PhD Dissertation, National Power Research and Technology Department, available from British Library Document Supply Center, DSC: DX172355.

Jing, Q., Pankratz, D., Princevac, M. and Venkatram, A. (2009) 'Modeling dispersion of buoyant releases in an urban area', Presented at *89th AMS Annual Meeting*, *11th Conference on Atmospheric Chemistry Special Symposium on Aerosol-Cloud-Climate Interactions*, January 2009, Phoenix, AZ.

Jing, Q., Venkatram, A., Princevac, M., Pankratz, D. and Qian, W. (2010) 'Modeling dispersion of buoyant emissions from low level sources in an urban area', Presented at *90th AMS Annual Meeting*, *16th Conference on Air Pollution Meteorology*, Atlanta, GA, January 2010.

Kulchin, Y.N., Voznesenskiy, S.S., Gamayunov, E.L., Gurin, A.S., Korotenko, A.A. and Maior, A.Y. (2007) 'An immersible fiber-optic fluorometer', Instruments and Experimental Techniques, Vol. 50, No. 6, pp.117–122.

Kychakoff, G., Howe, R.D. and Hanson, R.K. (1984) 'Quantitative flow visualization technique for measurements in combustion gases', *Applied Optics*, Vol. 23, No. 5, pp.704–712.

Macdonald, R.W., Griffiths, R.F. and Hall, D.J. (1998) 'A comparison of results from scaled field and wind tunnel modelling of dispersion in arrays of obstacles', *Atmospheric Environment*, Vol. 32, No. 22, pp.3845–3862.

Ohba, R., Kakishima, S. and Ito, S. (1990) 'Water tank study of plume rise and diffusion in a stably stratified layer under calm conditions', *Il NuovoCimentoC*, Vol. 13, No. 6, pp.1017–1028.

Petersen, R.L. and Beyer-Lout, A. (2012) 'AERMOD building downwash predictions – problems and solutions', *92nd AMS Annual Meeting, 17th Conference on Air Pollution Meteorology*, New Orleans, LA, January 2012.

Pournazeri, S. (2012) *Plume Rise and Dispersion of Emissions from Low Level Buoyant Sources in Urban Areas*, PhD dissertation, p.261, UMI Dissertation Services.

Pournazeri, S., Princevac, M. and Venkatram, A. (2012a) 'Scaling of building affected plume rise and dispersion in water channels and wind tunnels – revisit of an old problem', *Journal of Wind Engineering and Industrial Aerodynamics*, Vol. 103, pp.16–30, doi:10.1016/j.jweia. 2012.01.00.

Pournazeri, S., Princevac, M. and Venkatram, A. (2012b) 'Rise of buoyant emissions from low-level sources in the presence of upstream and downstream obstacles', *Boundary-Layer Meteorology*, Vol. 144, No. 2, pp.287–308.

Prasad, A.K., Adrian, R.J., Landreth, C.C. and Offutt, P.W. (1992) 'Effect of resolution on the speed and accuracy of particle image velocimetry interrogation', *Experiments in Fluids*, Vol. 13, Nos. 2–3, pp.105–116.

Princevac, M., Baik, J-J., Li, X., Park, S-B. and Pan, H. (2010) 'Lateral channeling within rectangular arrays of cubical obstacles', *Journal of Wind Engineering and Industrial Aerodynamic*, Vol. 98, pp.377–385.

Pringsheim, P. (1949) *Flourescence and Phosphorescence*, Interscience, New York.

Schulman, L.L., Strimaitis, D.G. and Scire, J.S. (2000) 'Development and evaluation of the PRIME plume rise and building downwash model', *Journal of the Air & Waste Management Association*, Vol. 50, No. 3, pp.378–390.

Snyder, W.H. (1981) *Guidelines for Fluid Modeling of Atmospheric Diffusion*, 200p, Report Number EPA-600/8-81-009, Environmental Protection Agency, Research Triangle Park, NC.

Snyder, W.H. (1985) 'Fluid modeling of pollutant transport and diffusion in stably stratified flows over complex terrain', *Annual Review of Fluid Mechanics*, Vol. 17, No. 1, pp.239–266.

Snyder, W.H. and Lawson Jr., R.E. (1994) 'Wind-tunnel measurements of flow fields in the vicinity of buildings', *8th AMS Conf. on Appl. Air Poll. Meteorol.*, AWMA, Nashville, Tennessee.

Venkatram, A., Pournazeri, S., Princevac, M., Pankratz, D. and Jing, Q. (2012) 'Dispersion of buoyant emissions from low level sources in urban areas', in *Air Pollution Modeling and Its Application XXI*, Vol. 4, pp.33–38, doi:10.1007/978-94-007-1359-8_6.

Yee, E., Gailis, R.M., Hill, A., Hilderman, T. and Kiel, D. (2006) 'Comparison of wind-tunnel and water-channel simulations of plume dispersion through a large array of obstacles with a scaled field experiment', *Boundary-Layer Meteorology*, Vol. 121, No. 3, pp.389–432.